73rd Conference of the Italian Thermal Machines Engineering Association (ATI 2018),
12–14 September 2018, Pisa, Italy

Analysis and Simulation of Non-Flamelet Turbulent Combustion in a Research Optical Engine

Clara Iacovano[a], Alessandro d'Adamo[b]*, Giuseppe Cantore[b]

[a]R&D CFD S.R.L., Via Vivarelli 2, Modena 41125, Italy
[b]Department of Engineering "Enzo Ferrari", University of Modena and Reggio Emilia, Via Vivarelli 10, Modena 41125, Italy

Abstract

In recent years, the research community devoted many resources to define accurate methodologies to model the real physics behind turbulent combustion. Such effort aims at reducing the need for case-by-case calibration in internal combustion engine simulations. In the present work two of the most widespread combustion models in the engine modelling community are compared, namely ECFM-3Z and G-equation. The interaction of turbulent flows with combustion chemistry is investigated and understood. In particular, the heat release rate characterizing combustion, and therefore the identification of a flame front, is analysed based on flame surface density concept rather than algebraic correlations for turbulent burn rate.

In the first part, spark-ignition (S.I.) combustion is simulated in an optically accessible GDI single-cylinder research engine in firing conditions. The turbulent combustion regime is mapped on the Borghi-Peters diagram for all the conditions experienced by the engine flame, and the consistency of the two combustion models is critically analysed.

In the second part, a simple test case is defined to test the two combustion models in an ideally turbulence-controlled environment: this allows to fully understand the main differences between the two combustion models under well-monitored conditions. and results are compared against experimental databases of turbulent burn rate for wide ranges of Damkohler (Da) and Karlovitz (Ka) numbers.

The joint experimental and numerical study presented in this paper evaluates different approaches within the unified flamelet/non-flamelet framework for modelling turbulent combustion in SI engines. It also indicates guidelines for reduced calibration effort in widespread combustion models.

* Corresponding author. Tel.: +39-0592056115; fax: +39-0592056126.
  E-mail address: alessandro.dadamo@unimore.it

Nomenclature

α	Calibration parameter of the flame surface density production in ECFM combustion model
$\tilde{c}$	Reaction progress variable in combustion models
c_p	Isobaric Specific Heat
Da	Damkohler number [-]
δ_L	Laminar flame thickness [m]
Δs	Difference between turbulent (s_T) and laminar (s_L) flame speed [m/s]
k	Turbulent Kinetic Energy [m^2/s^2]
Ka	Karlovitz number [-]
Le	Lewis number [-]
l^*	Efficiency function for unsteady flame kernel/turbulence interaction [-]
l_t	Integral Length Scale [m]
p / p_0	Absolute local/reference pressure [bar]
S.I.	Spark Ignition
s_L	Laminar flame speed [m/s]
s_T	Turbulent flame speed [m/s]
τ	Integral time scale $\tau = k/\varepsilon$ [s]
T / T_0	Absolute local/reference temperature [K]
u'	Turbulent intensity [m/s]
Y_{res}	Dilution mass fraction [-]

1. Introduction

The structure of turbulent flames in internal combustion engines is correlated to laminar and turbulent parameters, such as laminar flame speed, turbulent intensity and its temporal and spatial scales. They affect the turbulent burning velocity, which is ultimately related to the available torque output, fuel consumption and pollutant formation. The complex interplay of these phenomena complicates the required simulation effort for combustion models. These need to replicate the correct turbulent flame speed in a variety of length and velocity scale ratios between turbulence and chemistry (l_t/δ_L and u'/s_L, respectively), as depicted in the Borghi-Peters diagram for turbulent combustion [1]. In particular, the dimensionless Damkohler and Karlovitz numbers (Da and Ka) identify different combustion regimes, synthetically describing a variety of turbulence/flame interactions. The most widespread combustion models used for engine combustion are developed assuming a flamelet combustion regime for S.I. combustion, in which turbulence can only corrugate and extend the flame front surface preserving the inner laminar structure and flame speed (s_L). For this condition $Da > 1$ and $Ka < 1$. Despite this is generally verified for fully developed flames, the spatial distribution and temporal rapid variation of turbulent conditions potentially lead to different turbulence/chemistry interactions, e.g. small eddies might penetrate into the pre-reaction zone and expand it (thin reaction regime, $Da > 1$ and $Ka > 1$). Therefore, it is a fundamental requirement for combustion models to be able to simulate the correct turbulent flame speed (s_T) in all the potentially experienced combustion regimes. The combustion models discussed hereafter are ECFM-3Z and G-equation, which are among the most popular models used in the engine simulation community; while in the latter an explicit expression for s_T is needed for the "G" transport equation, in the former the effective s_T is obtained through a so-called Flame Surface Density equation. Both models have been extensively adopted in the engine community, thus emerging as alternative leading concepts to understand and improve S.I. combustion. The ECFM-3Z model was used by Lucchini et al. [2], where a sub-model for flame kernel growth was coupled to the ECFM-3Z model. The authors used ECFM-3Z in [3] to simulate the knock tendency of the same research engine presented hereafter; the combustion behaviour of gasoline and n-butanol was explained with ECFM-3Z in [4]. In [5-

7] a statistical knock model was presented, again coupled to the ECFM-3Z model. As for the G-equation model, it was used by Koch et al. in [8] to simulate spark-initiated combustion in a lean burn natural gas engine and in a small bore gasoline unit, testing two closure sub-models for s_T. Another successful application of the G-equation combustion model on a virtual CFR engine was carried out by Pal et al. [9], where the same burn rate and knock tendency as the experiments was obtained.

Within the G-equation context, several correlations for s_T from literature are tested in the present study, namely the Peters corr. (Eq. 1, [1]), the Gulder corr. (Eq. 2, [10]), the Bradley, Lau, Lawes corr. (Eq. 3, [11]) and the Ewald corr. (Eq. 4, [12]). They are used as a reference to identify a solid experimental basis for s_T trends as a function of local flow, mixture characteristics and Da number; the correlations are based on extensive sets of experimental campaigns under turbulence controlled conditions. In Figure 1 from [1] the experiments for s_T are normalized on the laminar flame speed (s_L) and u' to form the dimensionless group $\frac{\Delta s}{u'} = \frac{s_T - s_L}{u'}$, plotted as a function of Da. Despite the data scattering, in the low Da range a clear dependence of s_T on Da is observed, while in the high Da range turbulence is ineffective in further increasing the turbulent burning velocity due to promoted flame extinction: the asymptotic value of $\frac{\Delta s}{u'} \approx 1.8$ was found for all the considered campaigns, thus describing a universal feature of turbulent combustion.

Peters [1]: $\frac{\Delta s}{u'} = -\frac{a_4 b_3^2}{2b_1} Da + [(\frac{a_4 b_3^2}{2b_1} Da)^2 + a_4 b_3^2 Da]^{\frac{1}{2}}$, with $a_4 = 0.78$, $b_3 = 1$, $b_1 = 2$ (1)

Gulder [10]: $\frac{\Delta s}{u'} = 0.62 \cdot Da^{\frac{1}{4}}$ (2)

Bradley, Lau, Lawes [11]: $\frac{\Delta s}{u'} = 0.88 \left[0.157 \frac{u'}{s_L} \sqrt{\frac{\nu}{l_t \cdot u'}} Le \right]^{-0.3} - \frac{s_L}{u'}$ (3)

Ewald [12]: $\frac{\Delta s}{u'} = -\frac{a_4 b_3^2}{2b_1} Da \cdot l^{*(q+1)} + [(\frac{a_4 b_3^2}{2b_1} Da \cdot l^{*(q+1)})^2 + a_4 b_3^2 Da \cdot l^{*2}]^{\frac{1}{2}}$, with $a_4 = 0.78$, $b_3 = 1$,

$b_1 = 2$, $q = 2/3$, $l^* = \sqrt{1 - e^{(-2 \cdot \tau^*)}}$, $\tau^* = \frac{t_{comb}}{\tau}$, $\tau = \frac{k}{\varepsilon}$ (4)
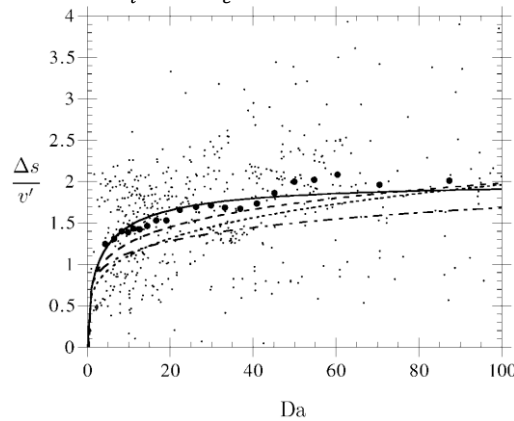

Fig. 1 Normalized turbulent flame speed variation $\Delta s/u'$ as a function of Damkohler number from [1].

As for s_L, the in-house developed methodology presented in [13, 14] is adopted for both combustion models. The method is based on a matrix of chemical kinetics simulations at engine-typical pressure and temperature, whose s_L results are fitted to obtain an algebraic yet chemistry-grounded correlation for the combustion models. The identified relationship is a 5th order logarithmic polynomial form (Eq. 5), and the reference values for pressure and temperature (P_0 and T_0) are 15 bar and 670 K, respectively. All the coefficients in Eq. 5 are from [14]. The effect of mixture dilution is accounted for as a linear scaling of the diluent mass fraction Y_{res} using a constant $f_{res} = 2.1$.

$$s_L = \left[\sum_{i=0}^{5} a_i \log(\phi)^i \right] \left(\frac{T}{T_0} \right)^{\sum_{i=0}^{5} b_i \log(\phi)^i} \left(\frac{P}{P_0} \right)^{\sum_{i=0}^{5} c_i \log(\phi)^i} (1 - f_{res} Y_{res})$$ (5)

The main advantage of this method is the possibility to overcome the limitations of common correlations for S_L (i.e. Metghalchi and Keck, Gulder, Rhodes, etc.), which were derived as fitting forms of combustion experiments conducted at largely different pressure and temperature from those experienced in engines. The extrapolation to higher pressure and temperature leads to relevant input errors for any combustion model.

2. Methodology

Engine combustion simulations are carried out using a customized version of STAR-CD licensed by SIEMENS PLM. A research engine with optical access through a transparent piston is chosen for model validations. Coherently with experimental practice, the Rassweiler-Withrow method is applied to the CFD results to calculate the burnt fraction based on time-dependent pressure and volume only. During the combustion simulations, mass-weighted average conditions are computed in the flame brush ($0.05 < \tilde{c} < 0.95$) at each iteration though user-coding, including turbulent and flame scales and key quantities. The adopted fuel is a surrogate of a commercial Gasoline, based on mean physical and chemical properties (e.g. saturation pressure, liquid/vapour density, H/C ratio, etc.). To reduce the computational effort, the computational grid reproduces half of combustion chamber with one intake and one exhaust port thanks to the geometrical symmetry of the engine (Figure 2a). The same engine operation with absolute intake pressure of 0.7 bar and intake air temperature of 310 K at 2000 rpm engine speed and stoichiometric mixture is used for all cases, the only variation being the combustion model. The spark time is fixed at -30 CA aTDC. The turbulent model used is the k-Epsilon/RNG with High Reynolds wall treatment and the GruMo-UniMORE wall function [15,16] for gas-to-wall heat fluxes. Wall temperatures are derived from a tuned 1D model and the values reported in Figure 2b are imposed as region-specific constant and uniform conditions. Time-varying pressure and temperature boundary conditions are applied at the intake and exhaust ports while an unsteady mass flow rate is applied at the bottom of cylinder to describe the blow-by effect through the piston rings. In addition to this, the experimental uncertainty of the effective compression ratio is overcome by preliminary simulations for motored operation, where the same trapping efficiency and mixture compression as the experimental test is reproduced. All the presented simulations share the mentioned setup, the only difference between the cases being the use of the ECFM-3Z combustion model (with $\alpha = 2$ for FSD production) and G-equation with s_T correlations from Eq. 1-4. Gasoline injection is modelled using a lagrangian approach and adopting a consolidated methodology for spray evolution described in [17].
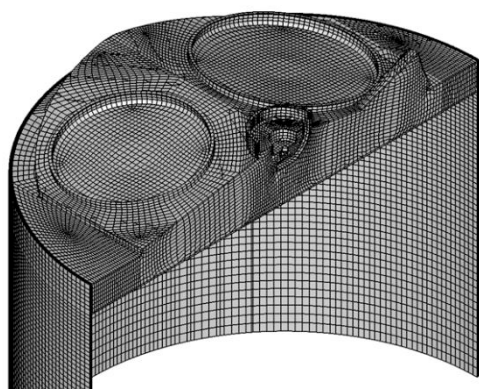
Engine Characteristics	
Displacement	400 cm³
Stroke	81.3 mm
Bore	79 mm
Compression ratio	9.8
Connecting rod length	143 mm
Dome wall temperature	200 °C
Piston wall temperature	320 °C
Liner wall temperature	150 °C
Intake port/valve wall temperature	100°C / 230°C
Exhaust port/valve wall temperature	130°C / 280°C

(a) (b)

Fig. 2 Single-cylinder 3D computational grid at TDC (a) and main engine characteristics (b).

As for the test case, a simple model is used to evaluate the two combustion models in a turbulence-controlled environment characterized by constant Da number; such condition is impossible in IC engine simulations because of the spatial and temporal changes in fluid dynamic conditions. A flame front evolution is simulated at a constant turbulence level with imposed laminar flame velocity and thickness (s_L and δ_L). Finally, the adoption of an open end at the burnt gas side ensures a constant pressure environment. Figure 3 shows the flame evolution in the 3D model

characterized by a pressure outlet, four symmetry planes on the tube sides to avoid any flame-wall effect and a closed wall end on the fresh mixture side. The flame propagates towards the zero-velocity fresh mixture while the burnt gases are accelerated and leave the domain through the pressure outlet boundary. The instantaneous flame front axial x-position is monitored at each iteration for the $\tilde{c} = 0.5$ iso-surface, and the turbulent flame speed for the model in use is evaluated as $s_T = \Delta x / \Delta t$ as illustrated in Figure 3, thanks to the null velocity of the fresh mixture side. This simple test case allows to precisely measure the effective s_T for any combustion model for any imposed turbulent and laminar conditions: therefore, it is possible to simulate any $\left(\frac{u'}{s_L}, \frac{l_t}{\delta_L}\right)$ point on the Borghi-Peters diagram and compare the model outcomes against correlations (Eq. 1-4) for an arbitrary combustion regime.
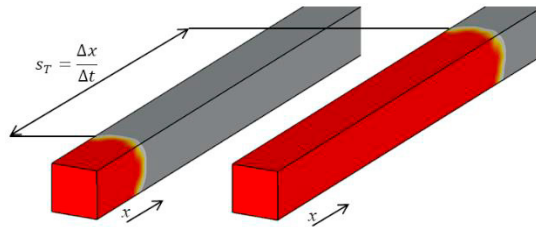

Fig.3 Combustion progress variable $\tilde{c}$ for two time stations and s_T calculation method.

3. Results

The comparison between experimental and simulated pressure traces and burnt fraction profiles are shown in Figure 4. To the aim of verifying the turbulent burn rate for both combustion models, the numerical results are obtained without calibration tuning. A marked dependency on the adopted correlation for s_T can be observed for the G-equation model, the ECFM-3Z being close to the Bradley correlation apart from a slightly delayed flame propagation. Generally speaking, the results are in good agreement with the experimental ensemble average traces for all models, with minor discrepancies which might be reduced with ad-hoc tuning. However, as the aim of this paper is to investigate the model response to a variety of turbulence/flame interaction in a S.I. engine, the study is conducted on the presented results without additional calibration.
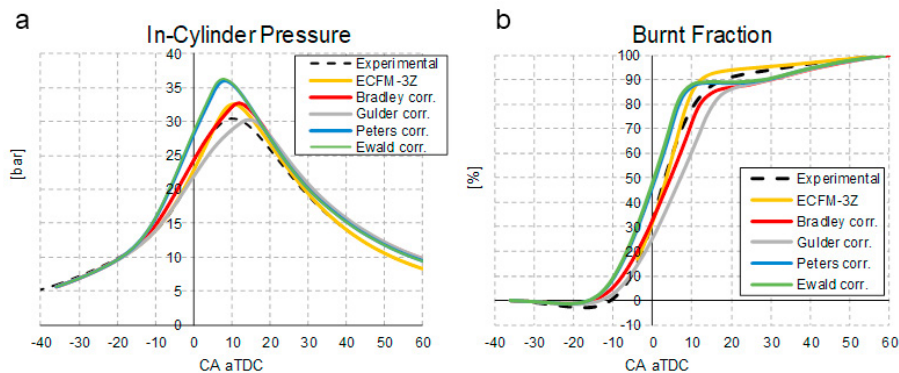

Fig. 4 (a) Pressure traces; (b) Evaporated fuel burnt trends (%).

In Fig. 5 the average $\left(\frac{u'}{s_L}, \frac{l_t}{\delta_L}\right)$ traces from CFD simulations are reported on the Borghi-Peters diagram for all models. Due to the different ignition treatment, the ECFM-3Z model locates the flame kernel inception in the thin reaction zone (non-flamelet condition); the flame reaches the flamelet condition before MFB5 (the $Ka > 1$ limit is experienced at -16 CA aTDC) and it abandons such regime after MFB90. As for the G-equation model, the flame kernel starts in the stirred reaction regime ($Da < 1$ and $Ka > 1$) and it is still in the thin reaction zone at MFB5. The motivation for the different traces from the two combustion models is found in the different treatment of the flame brush, especially for the spatial extension of the reaction volume predicted by the two models. Therefore, the mean turbulence/flame

interaction for the two models undergoes notable deviations despite the relatively similar global burn rate, due to different cell populations in the flame region and related distribution of chemistry and turbulent scales. This is shown by the scatter plots in Fig. 6, where the dispersion of states at MFB5/50 is reported for the two models: such observation emphasizes the requirement for combustion models to be predictive on all the potentially experienced combustion regimes. Figure 7 clarifies the different flame brush volume (identified using the $\tilde{c} \cdot (1 - \tilde{c})$ function) computed by the two models.
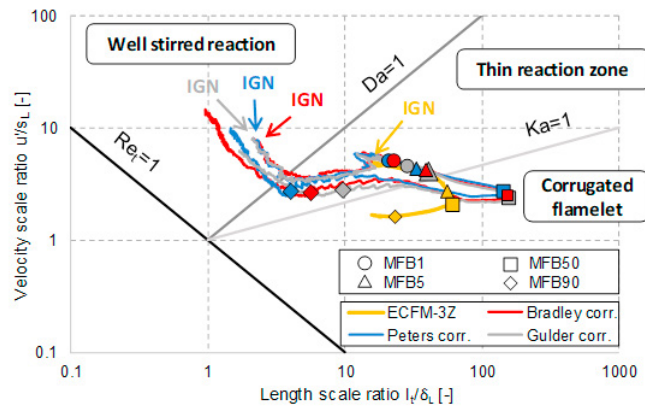

Fig. 5 Flame development to Borghi-Peters diagram with ECFM-3Z and G-equation models. Results from the Ewald corr. for s_T are omitted as superimposed to the Peters corr. ones.
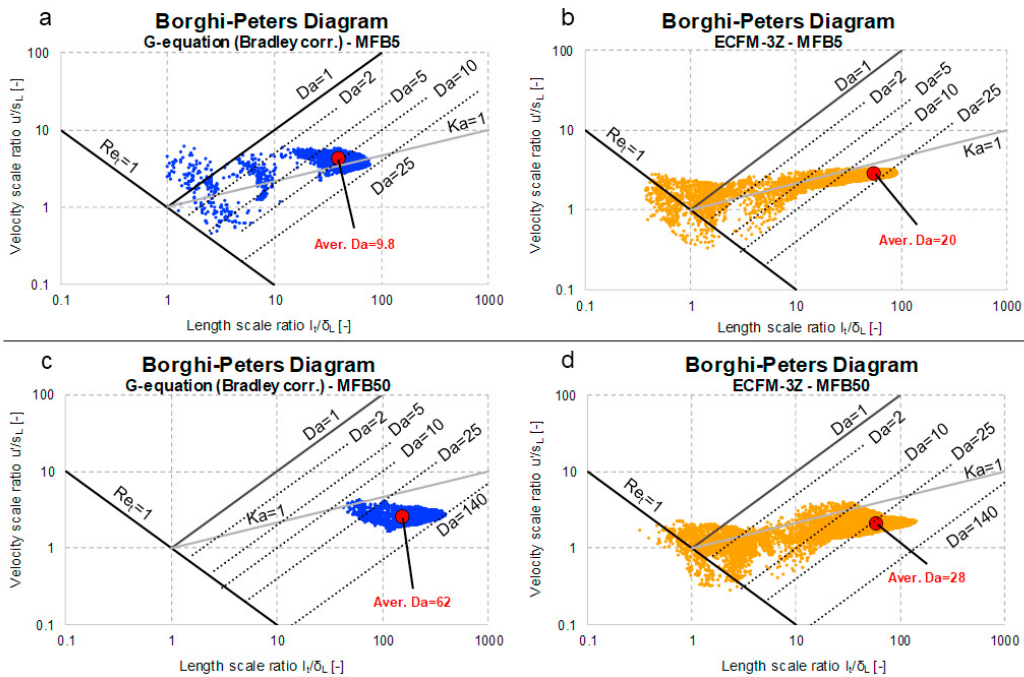

Fig. 6 Dispersion of local turbulence/flame interaction on the flame brush ($0.05 < \tilde{c} < 0.95$) at MFB5 using (a) G-equation with Bradley corr. for s_T and (b) ECFM-3Z. The same comparison is reported at MFB50 using (c) G-equation with Bradley corr. for s_T and (d) ECFM-3Z.

To check the predictive capabilities of the models at different combustion regimes, the same turbulence/flame interaction as the one experienced at MFB5 and MFB50 is reproduced using the presented test case. Results are reported in Fig. 8, together with the mean Da and Ka numbers experienced by the flame. The turbulence/flame interaction from this analysis is used as initial condition for the simplified test case, and results are reported in Fig. 9 in terms of the dimensionless groups Da and $\Delta s/u'$. Unlike engine simulations, a faster combustion is obtained with

ECFM-3Z compared to the G-equation model, while this last is in agreement with the experiment-based correlations used for s_T. This example emphasizes that relevant differences between the two models are present when testing selected $\left(\frac{u'}{s_L}, \frac{l_t}{\delta_L}\right)$ conditions, despite the overall good agreement between the two in terms of average burn rate. Such effect is ultimately due to the wide range of Da and turbulence/flame interactions. Therefore, the global burn rate is only a partial indication of the correctness of the simulation framework in terms of turbulent flame speed s_T, since combustion models need to account for a very wide variation of flow/chemistry interactions. In this context, the G-equation model combustion family emerges as a more promising universal approach for turbulent combustion in modern internal combustion engines operating under flamelet and non-flamelet regimes.
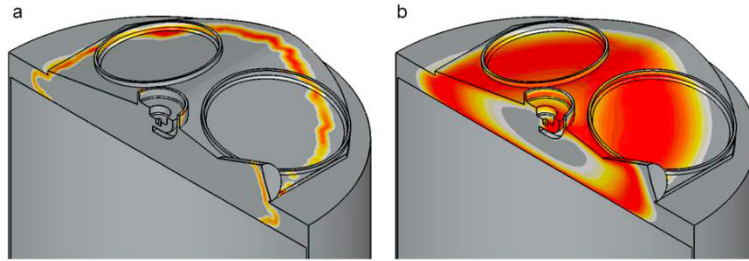

Fig. 7 Flame brush volume $\tilde{c} \cdot (1 - \tilde{c})$ at TDC for (a) G-equation and (b) ECFM-3Z.
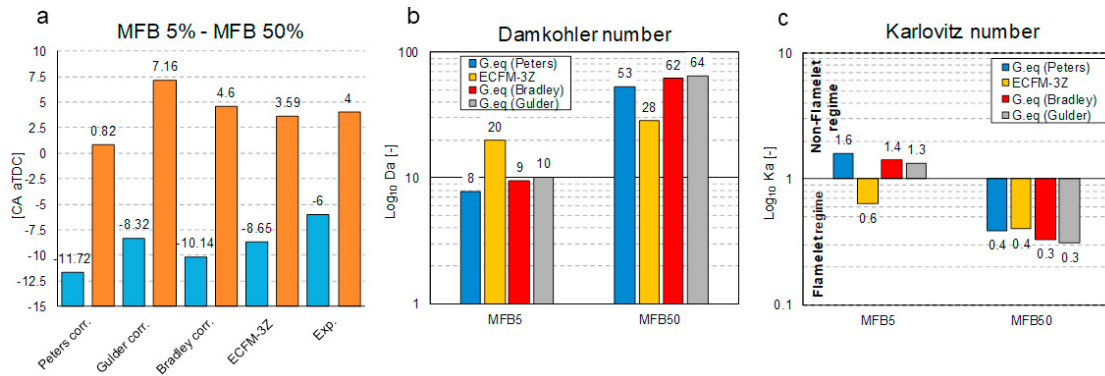

Fig. 8 (a) Combustion phasing for MFB5 and MFB50 obtained with all combustion models and experiments; (b) Damkohler numbers and (c) Karlovitz numbers at MFB5 and MFB50 of numerical simulations.
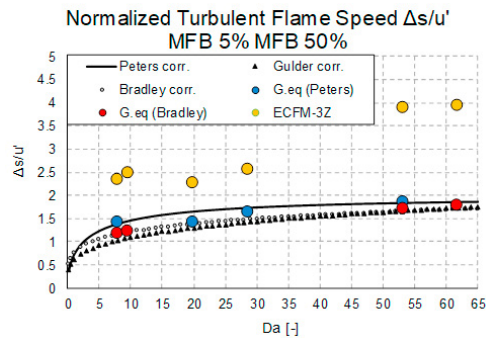

Fig. 9 Normalized turbulent flame speed at MFB5 and MFB50 from test case simulations with G-equation and ECFM-3Z model.

4. Conclusion

In the present work two widespread combustion models used in the engine industry (G-equation and ECFM-3Z) are compared and the turbulence/flame interaction under flamelet and non-flamelet conditions is investigated.

Combustion in a S.I. engine is simulated in an optically accessible GDI research engine in firing conditions. Results from both combustion models reasonably agree with the measured pressure trace and burn rate. The mean turbulence/flame interaction experienced by engine flames is reported on the Borghi-Peters diagram, confirming the occurrence of multiple regimes during the S.I. combustion. Scatter plots showing the dispersion of states at MFB5/50 emphasize the requirement for combustion models to be predictive on all the potentially present combustion regimes. In the part second of the paper a simple test case is adopted to assess the turbulent flame speed simulation in a turbulence-controlled environment, with the aim to fully elucidate difference and similarities between the two models and the experimental evidence. The obtained results are in contradictions with the burn rate from engine simulations: in these last, a variety of length and velocity scales simultaneously co-exist (i.e. Da and Ka ranges), and a satisfactory mean burn rate does not necessarily guarantee the model accuracy for any experienced turbulent/flame condition (e.g. near the walls). The proposed test case allows to investigate the simulated flame speed in any arbitrary point on the Borghi-Peters diagram, hence to test combustion models in both flamelet and non-flamelet regimes. The results from the G-equation model are in agreement with the experimental correlations on all the simulated Da representing the mean turbulence/flame interaction at MFB5/50, while ECFM-3Z results show relevant deviations from the target value in both cases. These results indicate the G-equation as a suitable model for both flamelet and non-flamelet conditions, thus promisingly targeting the challenging task of predictive engine combustion simulation.

References

[1] Peters Norbert, "Turbulent Combustion." *Cambridge University Press*, 2000.

[2] Lucchini, Tommaso, Cornolti, Luca, Montenegro, Gianluca, D'Errico, Gianluca. et al., "A Comprehensive Model to Predict the Initial Stage of Combustion in SI Engines." SAE Technical Paper 2013-01-1087, 2013, https://doi.org/10.4271/2013-01-1087

[3] Breda, Sebastiano, d'Adamo, Alessandro, Fontanesi, Stefano, Giovannoni, Nicola et al., "CFD Analysis of Combustion and Knock in an Optically Accessible GDI Engine." *SAE Int. J. Engines* 9(1):641-656, 2016, https://doi.org/10.4271/2016-01-0601.

[4] Breda, Sebastiano, d'Adamo, Alessandro, Fontanesi, Stefano, D'Orrico, Fabrizio et al., "Numerical Simulation of Gasoline and n-Butanol Combustion in an Optically Accessible Research Engine," *SAE Int. J. Fuels Lubr.* 10(1):32-55, 2017, https://doi.org/10.4271/2017-01-0546.

[5] d'Adamo, Alessandro, Breda, Sebastiano, Fontanesi, Stefano, and Cantore, Giuseppe, "A RANS-Based CFD Model to Predict the Statistical Occurrence of Knock in Spark-Ignition Engines," *SAE Int. J. Engines* 9(1):618-630, 2016, https://doi.org/10.4271/2016-01-0581.

[6] d'Adamo, Alessandro, Breda, Sebastiano, Fontanesi, Stefano, Irimescu, Adrian, Merola, Simona Silvia, Tornatore, Cinzia, "A RANS knock model to predict the statistical occurrence of engine knock.", *Applied Energy*, Volume 191, 1 April 2017, Pages 251-263

[7] d'Adamo, Alessandro, Breda, Sebastiano, Iaccarino, Salvatore, Berni, Fabio et al., "Development of a RANS-Based Knock Model to Infer the Knock Probability in a Research Spark-Ignition Engine." *SAE Int. J. Engines* 10(3):722-739, 2017, https://doi.org/10.4271/2017-01-0551.

[8] Koch, Jann, Xu, Guoqing, Wright, Yuri Martin, Boulouchos, Konstantinos et al., "Comparison and Sensitivity Analysis of Turbulent Flame Speed Closures in the RANS G-Equation Context for Two Distinct Engines," *SAE Int. J. Engines* 9(4):2091-2106, 2016, https://doi.org/10.4271/2016-01-2236.

[9] Pal, Pinaki, Kolodziej, Christopher P., Choi, Seungmok, Som, Sibendu, Development of a Virtual CFR Engine Model for Knocking Combustion Analysis," *SAE Technical Paper* 2018-01-0187, DOI: https://doi.org/10.4271/2018-01-0187

[10] Gulder, Omer L., "Turbulent premixed flame propagation models for different combustion regimes" *The Comb. Institute*, 1990/pp. 743-750.

[11] Bradley, Derek, Lau, A.K.C., Lawes, Malcolm, "Flame stretch rate as a determinant of turbulent burning velocity." *Phil. Trans. R. Soc. Lond.* (1992) 338, 359-387.

[12] Ewald, Jens, Peters, Norbert, "On unsteady premixed turbulent burning velocity prediction in internal combustion engines", *Proceeding of the Combustion Institute* 31 (2007) 3051-3058;

[13] d'Adamo, Alessandro, Del Pecchia, Marco, Breda, Sebastiano, Berni, Fabio et al., "Chemistry-Based Laminar Flame Speed Correlations for a Wide Range of Engine Conditions for Iso-Octane, n-Heptane, Toluene and Gasoline Surrogate Fuels," *SAE Technical Paper* 2017-01-2190, 2017.

[14] Del Pecchia, Marco, Breda, Sebastiano, d'Adamo, Alessandro, Fontanesi, Stefano et al., "Development of Chemistry-Based Laminar Flame Speed Correlation for Part-Load SI Conditions and Validation in a GDI Research Engine," *SAE Technical Paper* 2018-01-0174, 2018, https://doi.org/10.4271/2018-01-0174.

[15] Berni, Fabio, Fontanesi, Stefano, Cicalese, Giuseppe, and d'Adamo, Alessandro, "Critical Aspects on the Use of Thermal Wall Functions in CFD In-Cylinder Simulations of Spark-Ignition Engines," *SAE Int. J. Commer. Veh.* 10(2):547-561, 2017.

[16] Cicalese, Giuseppe, Berni, Fabio, Fontanesi, Stefano, d'Adamo, Alessandro et al., "A Comprehensive CFD-CHT Methodology for the Characterization of a Diesel Engine: from the Heat Transfer Prediction to the Thermal Field Evaluation," *SAE Technical Paper* 2017-01-2196, 2017, https://doi.org/10.4271/2017-01-2196.

[17] Postrioti, Lucio, Cavicchi, Andrea, Brizi, G., Berni, F. et al., "Experimental and Numerical Analysis of Spray Evolution, Hydraulics and Atomization for a 60 MPa Injection Pressure GDI System," *SAE Technical Paper* 2018-01-0271, 2018, https://doi.org/10.4271/2018-01-0271